Advanced Electronic Tongue Concept[1]

Martin G. Buehler, Gregory M. Kuhlman, and Didier Keymeulen
Jet Propulsion Laboratory, California Institute of Technology
and
Samuel P. Kounaves, Department of Chemistry. Tufts University

Abstract—-This effort, directed at developing a sensor for evaluating water quality, is based on electrochemical techniques that detect and identify ions in solution. This paper discusses the use of Cyclic Voltammetry (CV), corrosion measurements, and Anodic Stripping Voltammetry (ASV) to measure three marker ions Cu, Fe, and Zn using Electronic Tongue 1. Use of genetic algorithms are suggested as an approach to facilitate the search for optimum measurement conditions. In addition, the possibility of changing the physical conditions of the sample chamber is discussed as a way of increasing the sensor's apparent sensitivity of and confidence in the measurements.

TABLE OF CONTENTS

1. INTRODUCTION

This paper extends the work reported at last year's IEEE Aerospace conference where the design principles for the fabrication of Etng1 (Electronic Tongue No. 1) [Buehler, 2001] were discussed. In this effort the capabilities of Etng1 are explored using three sets of electrochemical measurements including Cyclic Voltammetry (CV) [Kissinger, 1996], corrosion measurements [Stansbury, 2000], and Anodic Stripping Voltammetry (ASV) [Wang, 2000]. This effort is an outgrowth of the 25-cm^3 electrochemical cell developed for the MECA (Mars Environmental Compatibility Assessment) project [West, 1999] which included 20 prefabricated Ion Selective Electrodes, a conductivity sensor, a temperature sensor and

an oxidation reduction potential sensor. Traditional electrochemical sensors are fabricated at the end of a pencil-like cylindrical tube. Such sensors cannot be configured easily in a multi-sensor array nor can they be miniaturized.

This is a joint effort between JPL, Tufts University, and ThermoOrion Research, Inc. Its goal is the development of a water quality sensor for use on the International Space Station Alpha and Martian habitate. The target ions are K^+ (340 mg/L), Ca^{2+} (30 mg/L), Mg^{2+} (50 mg/L) and Cl^- (200 mg/L) which represent some of the NASA Spacecraft Maximum Contaminant Levels (MCL) for potable water for International Space Station Alpha.

2. EXPERIMENTAL APPARATUS

The working electrodes (WE) and reference electrodes (RE) used in this effort were fabricated on ceramic substrates as seen in Fig. 1.
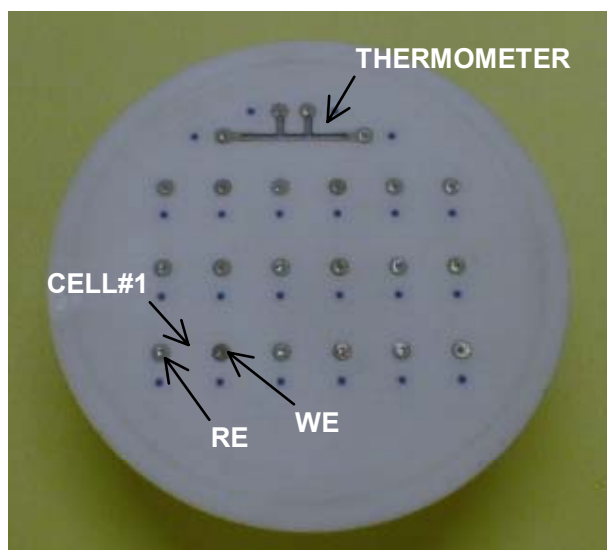

Figure 1. Top side of a 4.5-cm diameter ceramic substrate showing the working (WE) and reference (RE) electrodes arranged on a 3 × 3 array and a four-terminal thermometer.

The electrodes are arrayed in a 3×3 matrix. Each cell has one WE and RE electrode. The thermometer is formed by screen printing RuO_2 and is used to monitor the temperature of the solution. Two types of electrodes were screen printed onto the 1-mm thick 96%-pure alumina substrate. The first WE and RE electrodes were fabricated using Pd(12%)Ag(88%) and the second type with Au. After screen printing the electrodes were fired in air at 840°C. The electrodes are accessed using 0.5-mm diameter pins mounted on the underside of the substrate.

The substrate is mounted in the apparatus shown in Fig. 2a. The top of the chamber contains an array of nine Au/Ni plated Cu auxiliary electrodes (AE) located above the WEs. The distance between the WE and AE is about 2 mm. The volume of the chamber is about 1.5 mL.
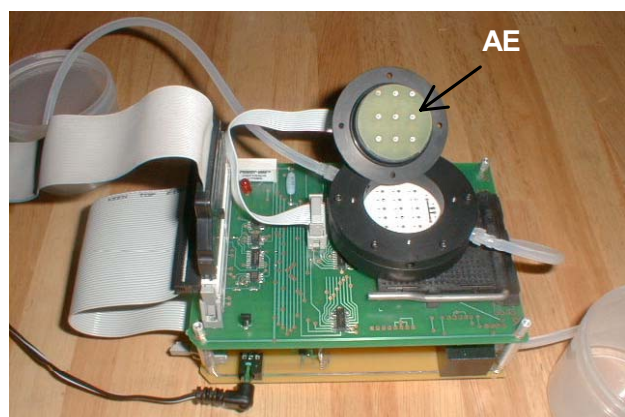

Figure 2a. Etng1 experimental apparatus showing the sample chamber exposed and the nine AEs located in the cap of the chamber.
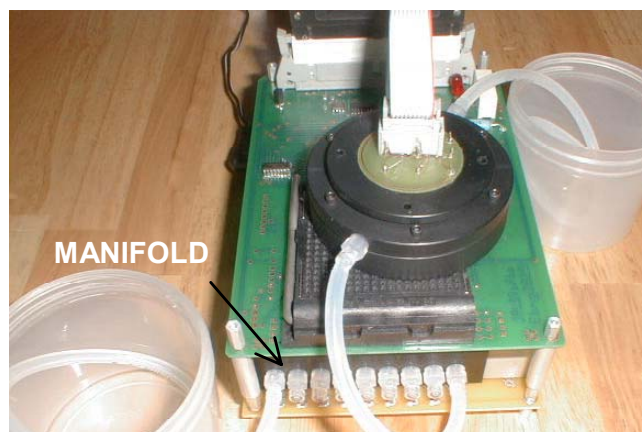

Figure 2b. Etng1 showing the eight-port manifold mounted on the lower fluidics board.

A further view of the apparatus is seen in Fig. 2b that shows the sample chamber mounted on an electronics board which is mounted above a fluidics board. The fluidics board includes an eight-port a manifold. Thus, eight reagents can be introduced into the chamber either one at a time or in mixtures by controlling the valves (not shown) located above the manifold.

The final view of the apparatus, shown in Fig. 2c, depicts the miniature 50-µL pump. The pump is operated at 3 Hz and so is capable of filling the 1.5 mL chamber in 10 s.
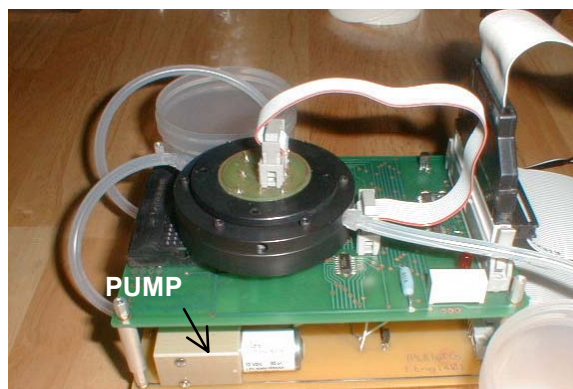

Figure 2c. Etng1 showing the 50-µL pump mounted on the lower fluidics board.

3. ELECTRONICS

Various solutions were measured using the three electrode potentiostat shown in Fig. 3 [Kissinger, 1996]. The electronics forces a voltage between the WE and RE to be at voltage determined by DAC0. This is achieved using the operational amplifier U2 to force a current through AE so that the commanded voltage between the WE and RE is achieved. The current through the addressed cell is determined from the voltage drop across R0. The main current flow is indicated for Cell#2 by the red (heavy) line in Fig. 3. The voltage between WE and RE is VWR and the voltage between the AE and RE is VAR.

4. EXPERIMENTS

The apparatus was characterized using four 0.1% by weight salt solutions of CuSO4, ZnSO4, and Fe2SO4. Prior to exposure to these salts, the chamber was filled with deionized water and the electrodes biased using our standard bias profile described below and this routine preconditions the electrodes. The solutions were characterized using CV measurements with a triangle wave voltage with a slope of ±0.1 V/s. One hundred stepped voltages formed the triangle wave that varied from +1.0 V to −1.2 V and back to +1.0 V. Two cycles were measured to demonstrate repeatability. Then ASV behavior was measured using a positive going voltage ramp where the ramp has 50 steps and a slope of +0.1 V/s. The linear ramp

was varied from –1.2 V to +1.0 V. Prior to the onset of this ramp the potential was held at –1.2 V for a deposition time of T_{dep}. This allowed the reduction of cations on the WE. During the ramp the cations are reoxidized at a potential characteristic of the cation. Again two traces were measured to demonstrate repeatability. The ASV results are used to relate the potential observed using our electrodes to results obtained using SHE (Standard Hydrogen Electrode).
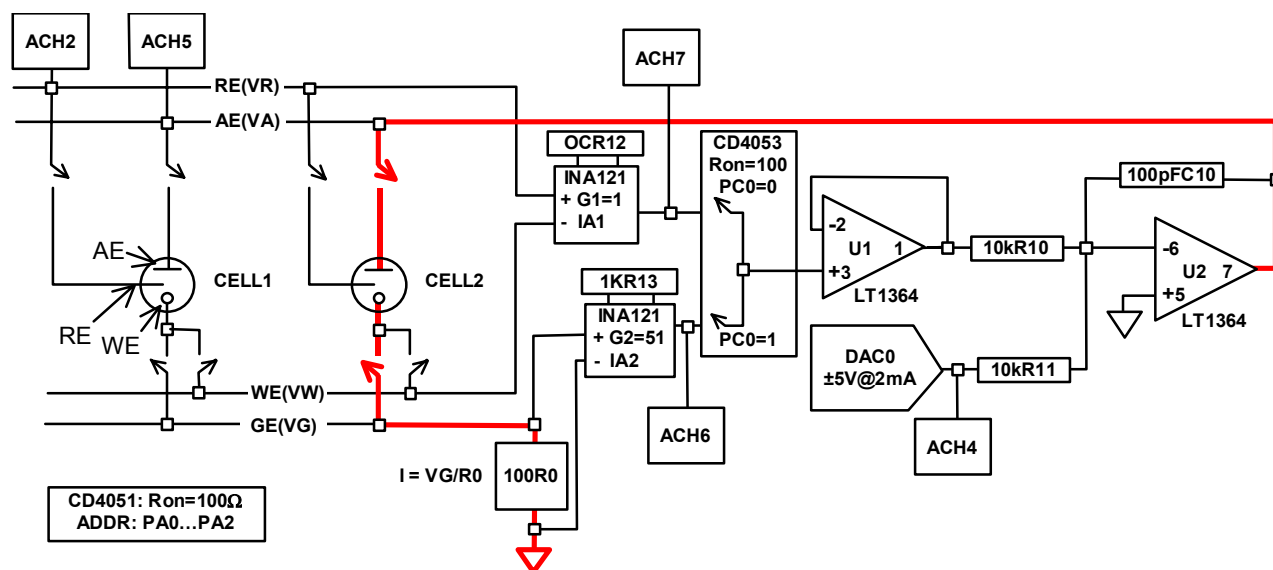

Figure 3. Etng1 potentiostat circuitry. Resistor values are in ohms. Ron is the MUX on resistance.

The results are shown in Figs. 5 to 7 and are organized as follows: CuSO4 is shown in Fig. 4, ZnSO4 in Fig. 5, and Fe2SO4 in Fig.6. Results for Au electrodes are shown in a, b, and c and results for PdAg are shown in d, e, and f. CV results are shown in a and d, Tafel results are shown in b and e, and ASV results are shown in c and f.

In the CV test results the open data (red curve) are VWR results and the solid data (blue curve) are VAR results. The CV curves provide insight into the nature of the chemical and electrochemical process occurring in the chamber [Kissinger, 1996]. During the negative going sweep (left to right) species in solution are reduced. During the positive going sweep (right to left) species in solution are oxidized. Species identification, however, is determined in subsequent analyses, in particular with ASV.

The CV data are replotted as Tafel curves. The open data (red curves) are oxidation results measured at the WE and the solid data (blue curve) are reduction results measured at the AE. The analysis of the corrosion data includes the intersection of the two curves which defines the corrosion potential, E_{corr}, and the corrosion current, I_{corr} [Stansbury, 2000]. In addition the voltages at zero current are designated as VAR(0) determined at the AE and VWR(0) determined at the WE.

ASV measurements are used to identify metals in solution. These measurements start at a negative potential of VWR = - 1.2 V where they are held for a deposition time, T_{dep} and

terminate at 1.0 V. The curves reveal anodic (negative going) peaks characteristic of ions being reoxidized from the WE into solution. In this study our goal is to detect marker ions in solution in order to characterize the response of the quasi Ag RE and relate the measured potentials to SHE (Standard Hydrogen Electrode) potentials. The ultimate goal is to use the ASV technique to detect very low levels (ppb [Wang2000]) of contaminates in water.

5. EXPERIMENTAL RESULTS

General observations of the results seen in Figs. 4 to 6 are as follows. The results obtained using Au or PdAg WE and RE are qualitatively the same. Also the repeatability of the two traces are quite good in that the second trace overlays the first trace. One must look closely to see differences.

The ASV response for the PdAg electrodes are shown in Figs. 4f, 5f, and 6f. The peak voltages are plotted in Fig. 7 against the V(SHE), Standard Hydrogen Electrode. The relationship between them is: V(PdAg) = V(SHE) –0.18. Also shown are results from the Au electrodes taken from Fig. 4c, 5c, and 6c. The Au electrodes do not have a straight-line relationship as does the PdAg electrodes. For comparison purposes, results are also shown in Fig. 7 for data taken at Tufts [Kovacs, 1995]: these results were measured using a Ag/AgCl RE and a ramp square wave
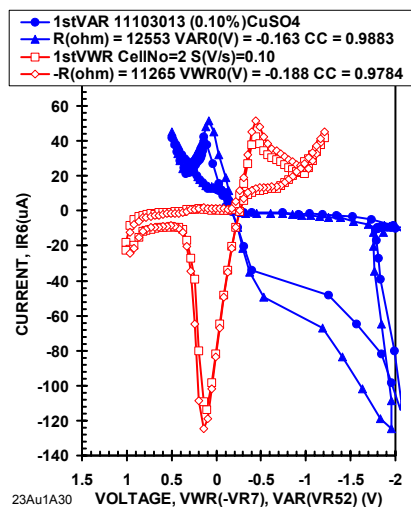
Figure 4a. CV CuSO$_4$ response for Au WE and RE.
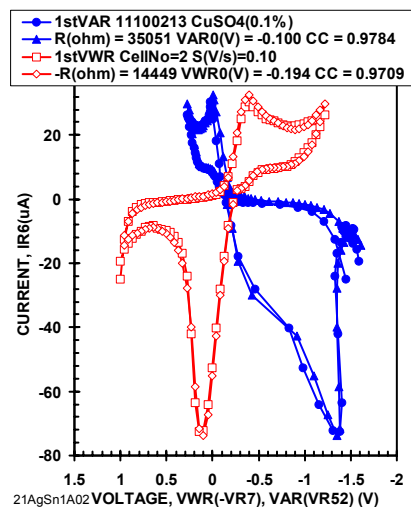
Figure 4d. CV CuSO$_4$ response for PdAg WE and RE.
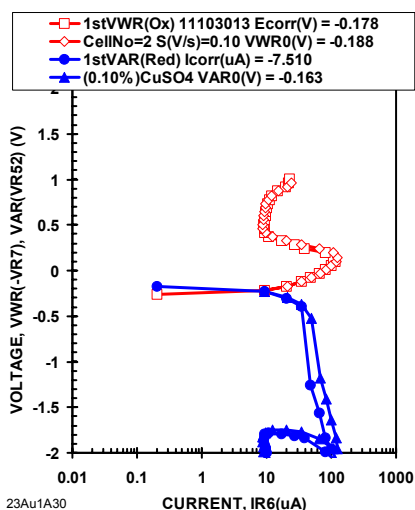
Figure 4b. Tafel CuSO$_4$ response for Au WE and RE.
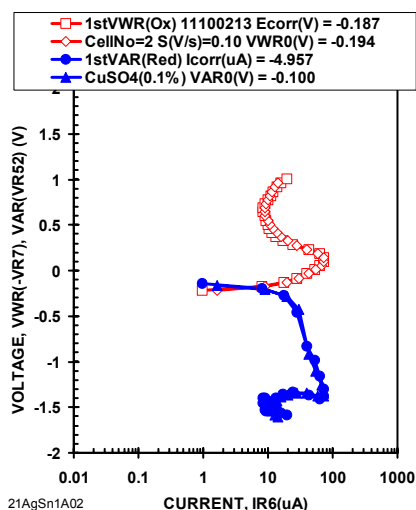
Figure 4e. Tafel CuSO$_4$ response for PdAg WE and RE.
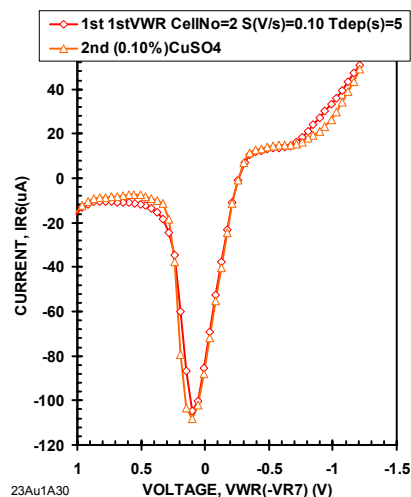
Figure 4c. ASV CuSO$_4$ response at a Au WE for T$_{dep}$ = 5 s. A negative going peak occurs at VWR = 0.1V.
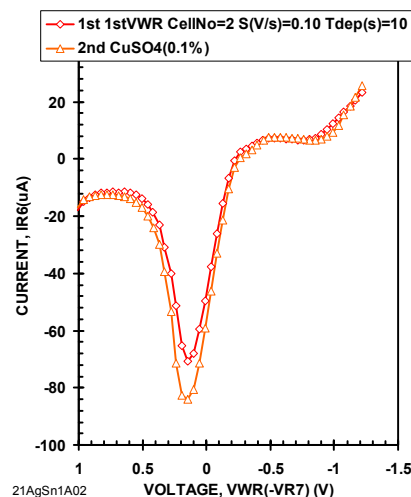
Figure 4f. ASV CuSO$_4$ response at a PdAg WE for T$_{dep}$ = 10 s. A negative going peak occurs at VWR = 0.16V.

4
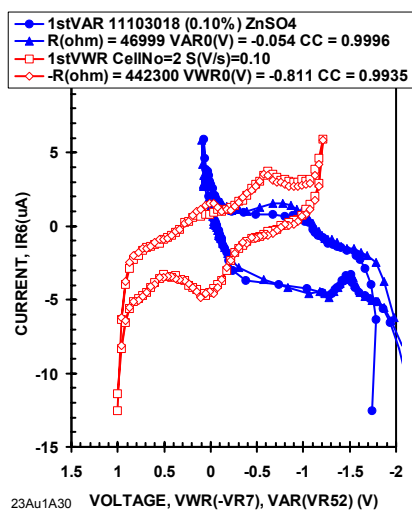
Figure 5a. CV ZnSO$_4$ response for Au WE and RE.
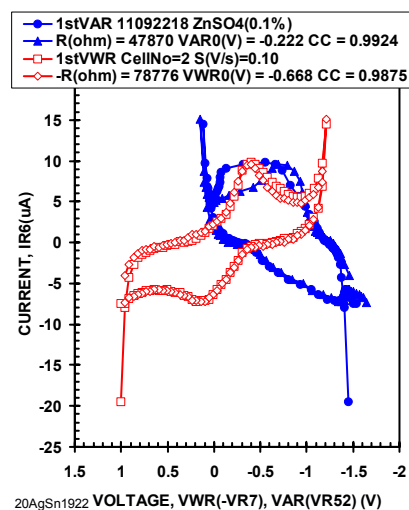
Figure 5d. CV ZnSO$_4$ response for PdAg WE and RE.
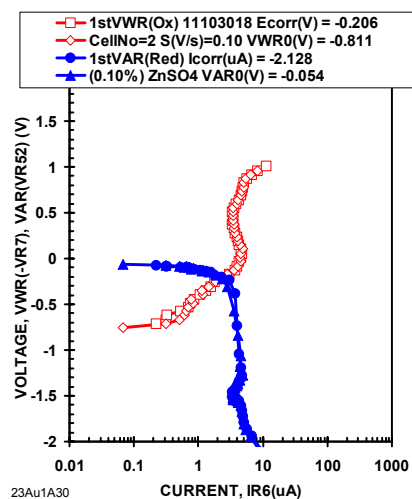
Figure 5b. Tafel ZnSO$_4$ response for Au WE and RE.
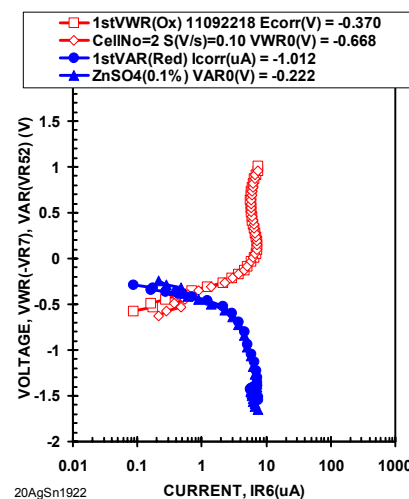
Figure 5e. Tafel ZnSO$_4$ response for PdAg WE and RE.
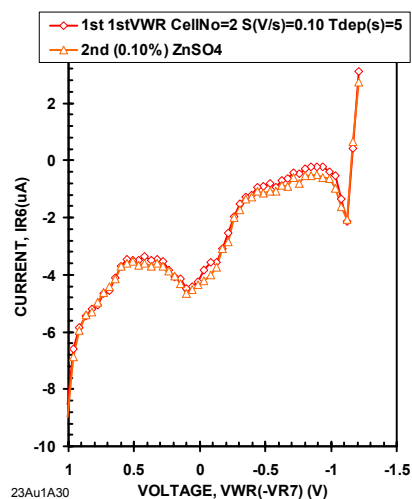
Figure 5c. ASV ZnSO$_4$ response at a Au WE for T$_{dep}$ = 5 s. A negative going peak occurs at VWR = -1.12V.
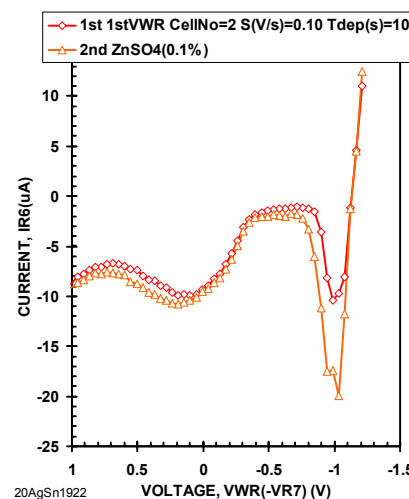
Figure 5f. ASV ZnSO$_4$ response at a PdAg WE for T$_{dep}$ = 10 s. A negative going peak occurs at VWR = -1.00V.
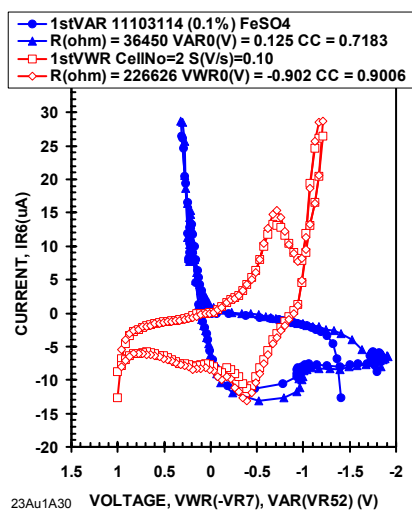
Figure 6a. CV FeSO$_4$ response for Au WE and RE.
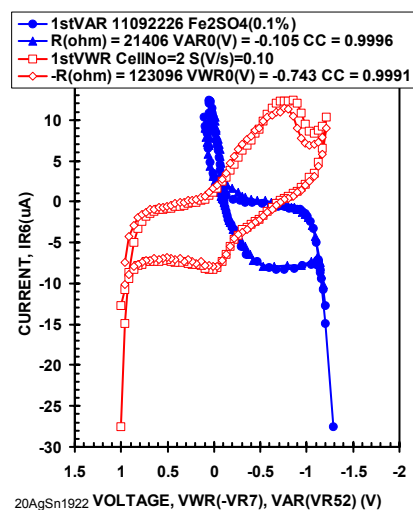
Figure 6d. CV FeSO$_4$ response for PdAg WE and RE.
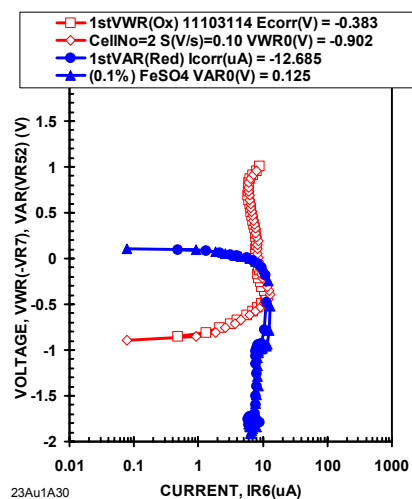
Figure 6b. Tafel FeSO$_4$ response for Au WE and RE.
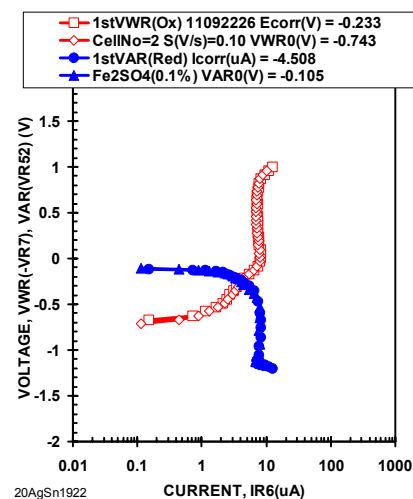
Figure 6e. Tafel FeSO$_4$ response for PdAg WE and RE.
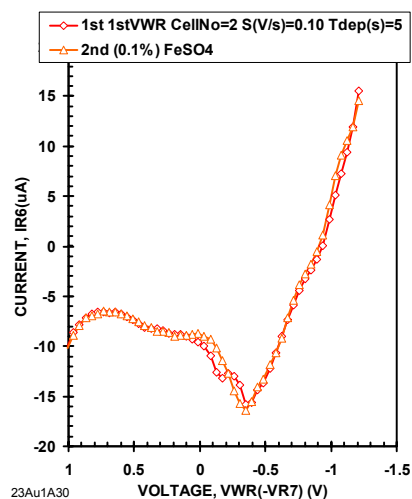
Figure 6c. ASV FeSO$_4$ response at a Au WE for T_{dep} = 5 s. A negative going peak occurs at VWR = -0.35.
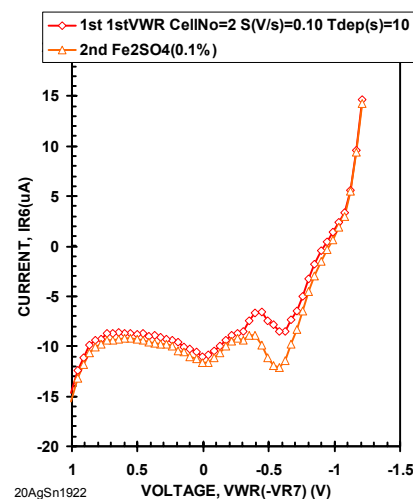
Figure 6f. ASV FeSO$_4$ response at a PdAg WE for T_{dep} = 10 s. A negative going peak occurs at VWR = -0.6V.

exciting signal; whereas, the results from this investigation used a quasi PdAg RE and a ramp step exciting signal.

All of the CV curves, seen in Figs. 4 to 6 have a positive going reduction current peak that occurs between –0.4 and –0.7 V. The common compound between the three solutions is the sulfate ion. Thus, the reduction peak is most-likely due to the sulfate reaction:

$$SO_4{}^{2-} + 4H^+ + 2e = H_2SO_3 + H_2O$$
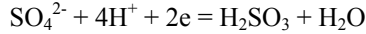
where $E° = +0.172$ V(SHE) = -0.006 V(PdAg). The negative going oxidation current peak, seen in Figs. 5a, 5d, 6a, and 6c is attributed to the reoxidation of the sulfate ion in the case of $ZnSO_4$ and the $FeSO_4$. For the case of the $CuSO_4$, the negative going response, seen in Figs. 4a and 4d, is due to both the oxidation of Cu reduced onto the WE during the negative bias portion of the CV curve and sulfate ion reduction. There is addition structure in the $ZnSO_4$ CV curve shown in Fig. 5a that is unexplained at this time.

The Tafel curves are a replot of the CV curves. Tafel curves are traditionally used to characterize the effects of corrosion on the WE. In these experiments the WE is either Au or PdAg where the $E°$ is +0.8 V(SHE) for Ag or +1.5 V(SHE) for Au. According to the Nernst relationship, these electrodes will oxidize (corrode) only when VWR is close to or above the $E°$ potential. Since the VWR(0) is less than zero volts, the shape of the oxidation curves (open red symbol) can not be attributed to the direct oxidation or dissolution of Au and PdAg into solution.

The Tafel oxidation curves (open red symbol) are explained by the same mechanism used to explain the oxidation portion of the CV curves. That is, the Tafel oxidation curves are due to the oxidation of the sulfate ion in the case of the $ZnSO_4$ and $FeSO_4$ electrolytes. For the case of the $CuSO_4$ electrolyte the oxidation curve is due to both the oxidation of the sulfate ion and the oxidation of the Cu reduced on to the WE during the negative voltage portion of the CV curve.

The Tafel reduction curves (closed black symbol) are most likely due to hydrogen reduction at the AE. Hydrogen generation produces the flat portion of the curve at low currents. At higher currents, the steep drop in the curve with voltage is due to diffusion-limited hydrogen evolution at the AE.

The Tafel curves are usually measured using very slow ramp voltages where currents in the cell reach a steady state value. In this experiment the exciting triangle wave had a slope of 0.1 V/s. This slope is fast enough to produce a CV curve with hysteresis which indicates that the cell has not reached equilibrium. Thus the Tafel curves shown here

are dynamic and not steady state measurements. Thus, these Tafel curves provide dynamic values for I_{corr} and E_{corr}.
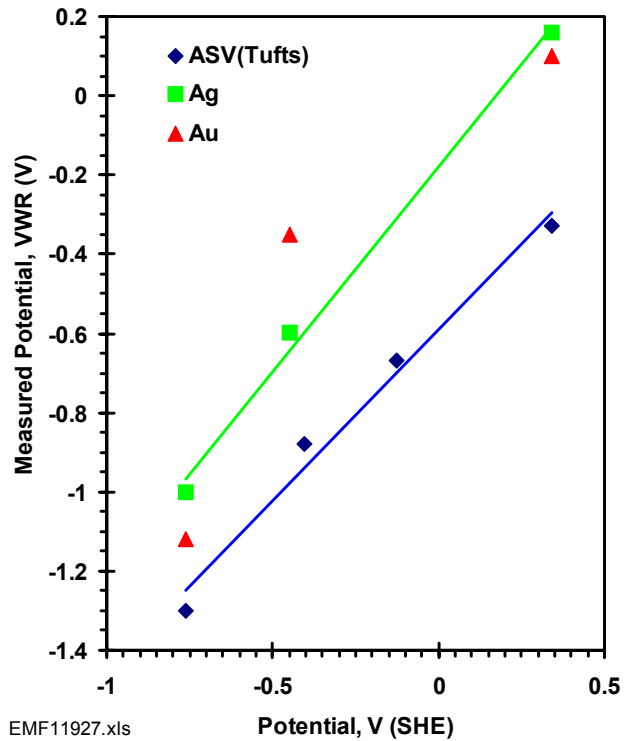

Figure 7. Response of Etng1 ASV peaks versus the SHE (standard hydrogen electrode) potential. Also shown are the ASV peaks reported by [Kovacs, 1995].

6. SENSOR CONTROL AND PATTERN MATCHING

These measurements have a large parameter space. For instance, the exciting signal, VWR, has a certain span (1.0 to –1.2 V), a sweep rate (0.1 V/s), waveform (triangle wave formed using steps versus pulses) and deposition time, T_{dep}. Likewise, the measured signals have a span and gain. The measurement conditions vary depending on the ion in solution and its concentration. In addition the chamber environment can be altered by changing temperature, adding oxygen (aerating) or nitrogen (deaerating), or by changing pH or adding complexing agents. Finally, the condition of the electrode surfaces, which can change with use, also influences the measurements. All of these factors contribute to the multi-parameter measurement space. For these reasons, the use of computer searching techniques is seen as essential to speeding progress during the development cycle, facilitating the search for optimum measurement conditions and increasing the apparent sensitivity and confidence in the measurements.

The approach to detecting contaminants in water is depicted in Figure 8. It is based on a Genetic Algorithm (GA) that has two purposes: (1) to optimize the pattern matching algorithm based on chemometric techniques and the immune system and (2) to design and select the optimal experimental parameters that control the conditions in the sample chamber. The genetic algorithm is used because it useful in high-dimensional search spaces and makes fewer assumptions about the search space than strong optimization method like gradient search. GA's use concepts gleaned from Darwin's theory of evolution by natural selection and also from the mechanisms involved in the alteration and transfer of genetic information to individuals in a population [Goldberg, 1989]. GA has been used by the Evolvable Hardware group at JPL for on-chip analog circuit optimization [Stoica, 2001], self-repaired circuit [Keymeulen, 2000] and optimal in-situ signal conditioning [Keymeulen, 2001].

Consider our immune system as functioning like a pattern recognition mechanism and the genetic algorithm as an investigation mechanism to search for impurities in water. Our immune system protects us from an extraordinary large variety of bacteria, viruses, and other pathogenic organisms. It also constantly surveys the body for the presence of abnormal cells, such as tumor cells and virally infected cells and destroys such cells when they are found. To perform these tasks the immune system must be capable of distinguishing good cells and molecules, which it should not be destroyed, from foreign cells and molecules (antigens), which should be destroyed. From an information-processing perspective, recognizing an almost limitless number of foreign cells and molecules, and distinguishing these from the good ones is a formidable task.
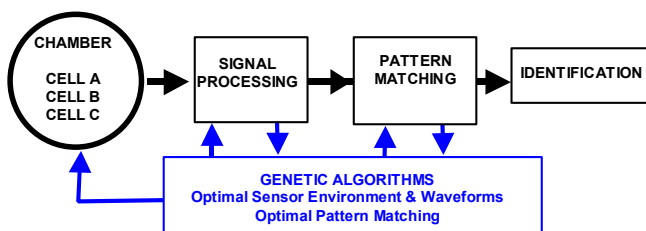

Figure 8. Sensor control and pattern matching using genetic algorithm.

In this effort models will mimic the pattern recognition process and learning that takes place in the immune system. Models have been developed and applied to the detection of computer viruses [Forrest, 1997] and novelty detection in time series data [Dasgupta, 1999]. There the virus must be detected and patterns recognized in unknown computer environments. We will apply the same strategy, as well as chemometric techniques, in our system to learn the signatures of known impurities in water and be able to differentiate from unknown impurities.

The genetic algorithm is also used to determine the optimal parameters that control the conditions found in the sample chamber. That is, after the initial signals from the sample chamber are detected, the results are analyzed by looking for matching patterns. The adaptive control then searches using a genetic algorithm for suggestions on how to modify the environment of the sample chamber or how to alter the signals used to measure the sensor. For example, the sample chamber environment can be altered by changing the temperature, altering the pH, or adding complexing reagents. The sensor waveform signals can be altered by changing the signal gain or by altering the parameters that determine the square-wave sweep parameters. Thus, the first answer can be refined to provide a more informed second answer. In this way we hope to be able to discriminate between contaminates in the water and increase the apparent sensitivity of the sensors.

7. CONCLUSION

This paper presented CV, Corrosion (Tafel) and ASV results from Etng1 using three marker ions: Cu, Fe, and Zn. The results illustrate the complexity of measurement conditions that involve: (a) exciting signal, (b) measured signal, (c) chamber environment, and (d) ion detected. The use of a genetic algorithm is seen as essential to speeding progress during the development cycle, facilitating the search for optimum measurement conditions and increasing the apparent sensitivity of and confidence in the measurements.

8. REFERENCES

M. G. Buehler, S. P. Kounaves, D. P. Martin, S. J. West, G. M. Kuhlman, "Designing a Water-Quality Monitor Using an Array of Ion Selective Electrodes", *2001 IEEE Aerospace Conference,* **2001***, Vol. 1,* 331-338.

D. Dagupta and S. Forrest. Artificial Immune Systems in Industrial Applications. In *Proc. of the Int Conf on Intelligent Processing and Manufacturing Material.* Honolulu, HI, July 10-14,1999.

S. Forrest et al. Computer Immunology. In *Communications of the ACM* Vol. 40, No. 10, pp. 88-96 (1997).

D. E. Goldberg, *Genetic Algorithms in Search, optimization and Machine Learning,* Addison-Wesley: Reading, MA, 1989.

D. Keymeulen, A. Stoica, R. Zebulum. Fault-Tolerant Evolvable Hardware using Field Programmable Transistor Arrays. In *IEEE Trans. on Reliability, Special Issue on Fault-Tolerant VLSI Systems*, vol. 49, No. 2, 2000. IEEE Press.

D. Keymeulen, R. Zebulum, A. Stoica, M. Buehler. Initial Experiments of Reconfigurable Sensor Adapted by Evolution. In *Proc. of Int Conf on Evolvable Systems,* October 3-5, 2001, Tokyo, Japan. Springer-Verlag.

P. T. Kissinger and W. R. Heineman, *Laboratory Techniques in Electroanalytical Chemical*, Marcel Dekker (New York, 1996).

G.T.A. Kovacs, C. W. Storment and S. P. Kounaves, Sensors and Actuators B, 23, 41-47, 1995

E. E. Stansbury and R. A. Buchanan, *Fundamentals of Electrochemical Corrosion*, ASM Int. (Materials Park, OH, 2000).

J. Wang, *Analytical Electrochemistry*, Wiley-VCH, New York, 2000.

S. J. West, X. Wen, R. Geis, J. Herdan, T. Gillette, M. H. Hecht, W. Schubert, S. Grannan, S. P. Kounaves, "Electrochemistry on Mars," American Laboratory 31 (20), p. 48–, Oct. 1999

9. ACKNOWLEDGMENTS

10. BIOGRAPHIES

Martin G. Buehler *received the BSEE and MSEE from Duke University in 1961 and 1963, respectively and the Ph.D. in EE from Stanford University in 1966 specializing in Solid State Electronics. He worked at Texas Instruments for six years, at National Bureau of Standards (now NIST) for eight years, and since 1981 has been at the Jet Propulsion Laboratory where he is a senior research scientist. At JPL he has developed p-FET radiation monitors for CRRES, Clementine, TELSTAR and STRV, E-nose which flew on STS-95, and an electrometer for the Mars '01 robot arm. Currently he serves on the staff of the New Millennium Program as a technical analyst. Martin is a member of the IEEE, Tau Beta Pi, and Sigma Nu. He holds 12 patents and has published over one hundred papers.*

Gregory M. Kuhlman: *Greg received a B.S. degree in Bacteriology from the University of Wisconsin-Madison in 1995. Following graduation Greg has worked for the University of Wisconsin-Madison, Covance Laboratories Incorporated, and Amgen Incorporated before coming to the Jet Propulsion Laboratory (JPL) in 2000. Greg's skills include classical bacteriology techniques, modern molecular biology techniques and extensive protein chemistry skills. Greg has mastered most modern chromatographic techniques such as High Pressure Liquid Chromatography (HPLC), Fast Protein Liquid Chromatography (FPLC) and Capillary Zone Electrophoresis (CZE). As an undergraduate at the University of Wisconsin-Madison Greg worked in the lab of Dr. Eric Johnson, world renown researcher of clostridium botulinum and other food borne pathogens, and has acquired the skills for working with pathogenic microorganisms. At JPL Greg focuses his time between two groups. He works with the Planetary Protection Technologies Group where he is researching and evaluating advanced technologies for molecular detection of microbes on spacecraft materials and in spacecraft assembly facilities. Greg also works with the Microdevices*

Laboratory where he is utilizing his biology skill set to test and study the effects of biofilms on space flight hardware.

Didier Keymeulen *received the BSEE degree from the Universite Libre de Bruxelles, Belgium, in 1987 and the MSEE and Ph.D. in Electrical Engineering and Computer Science from the Vrije Universiteit Brussels, Belgium in 1991 and 1994, respectively with the specialization in Artificial Intelligence. In 1995 he was the Belgium laureate of the Japan Society for the Promotion of Science Post Doctoral Fellowship for Foreign Researchers. In 1996 he joined the computer science division of the Japanese National Electrotechnical Laboratory as senior researcher. Since 1998, he is member of the technical staff of JPL in the Advanced Computing Technologies Group. At JPL, he is responsible for the applications of the DARPA project on evolvable hardware for adaptive computing that leads to the development of fault-tolerant electronics and autonomous and adaptive sensor technology. His expertise is in adaptive and learning hardware for autonomous systems. He is the author of over 30 papers covering topics in qualitative modeling for diagnostic and control of physical systems, adaptive and learning systems for mobile robot navigation and implementation of dynamical systems on massively parallel computers. He served as the co-chair of the NASA/DoD Workshop on Evolvable Hardware and served as its co-chair in 1999, program co-chair in 2000, and chairman in 2001. Didier is a member of the IEEE.*

Samuel P. Kounaves *received his BS/MS from Cal State - San Diego in 1976/78 and his Ph.D. (D.Sc.) from the University of Geneva in Switzerland in 1985. After a post-doctoral fellowships at SUNY-Buffalo and Harvard University he joined the faculty at Tufts University in 1988, where he is currently an Associate Professor of Chemistry. He has an active research group of 8 Ph.D. students and one undergraduate. He has been a principal investigator on more than 15 grants from government (NSF, EPA, DOE) and industry (PRF, EG&G, Orion). He has authored over 50 publications and holds 3 Patents. His research has been directed at the development of microfabricated electrochemical and chemically modified sensors, for use in monitoring and investigation of remote hostile environments, especially planetary bodies. Most recently he has been involved with NASA's Jet Propulsion Laboratory to include several sensor arrays on the next Mars Lander for performing chemical analysis of the Martian soil.*